Computational and Structural Biotechnology Journal 21 (2023) 5423–5433

Contents lists available at ScienceDirect

Computational and Structural Biotechnology Journal

journal homepage: www.elsevier.com/locate/csbj

Research article

Comprehensive bioinformatics analysis revealed potential key genes and pathways underlying abdominal aortic aneurysm

Kaijie Zhang [a], Jianing Yue [b], Li Yin [a], Jinyi Chen [a], Yunlu Chen [c], Lanting Hu [a], Jian Shen [d], Naiji Yu [a], Yunxia Gong [a], Zhenjie Liu [a,*]

[a] Department of Vascular Surgery, Second Affiliated Hospital of Zhejiang University School of Medicine, Hangzhou, Zhejiang Province 310009, China
[b] Department of Vascular Surgery, Zhongshan Hospital of Fudan University School of Medicine, Shanghai 200032, China
[c] Clinical Research Center, Second Affiliated Hospital of Zhejiang University School of Medicine, Hangzhou, Zhejiang Province 310009, China
[d] Department of Cardiology, Second Affiliated Hospital of Zhejiang University School of Medicine, Hangzhou, Zhejiang 310009, China

ARTICLE INFO

Keywords:
Abdominal aortic aneurysm
Comprehensive bioinformatics analysis
Key genes
ScRNA-seq analysis
RNA-seq analysis

ABSTRACT

Abdominal aortic aneurysm (AAA) is a permanent, asymptomatic segmental dilatation of the abdominal aorta, with a high mortality risk upon rupture. Identification of potential key genes and pathways may help to develop curative drugs for AAA. We conducted RNA-seq on abdominal aortic tissues from both AAA patients and normal individuals as a control group. Integrated bioinformatic analysis was subsequently performed to comprehensively reveal potential key genes and pathways. A total of 1148 differential expressed genes (DEGs) (631 up-regulated and 517 down-regulated) were identified in our study. Gene Ontology (GO) analysis revealed enrichment in terms related to extracellular matrix organization, while KEGG analysis indicated enrichment in hematopoietic cell lineage and ECM-receptor interaction. Protein-protein interaction (PPI) network analysis revealed several candidate key genes, and differential expression of 6 key genes (*CXCL8*, *CCL2*, *PTGS2*, *SELL*, *CCR7*, and *CXCL1*) was validated by Gene Expression Omnibus (GEO) datasets. Receiver operating characteristic curve (ROC) analysis demonstrated these genes' high discriminatory ability between AAA and normal tissues. Immunohistochemistry indicated that several key genes were highly expressed in AAA tissues. Single-cell RNA sequencing revealed differential distribution patterns of these identified key genes among various cell types. 26 potential drugs linked to our key genes were found through DGIdb. Overall, our study provides a comprehensive evaluation of potential key genes and pathways in AAA, which could pave the way for the development of curative pharmacological therapies.

1. Introduction

Abdominal aortic aneurysm (AAA) is an inflammatory disease characterized by a persistent segmental dilation of the abdominal aorta. According to the latest investigation by the American Heart Association (AHA), the incidence of AAA among males aged 75–84 was 12.5%, while among females, it was 5.2% [1]. Established AAA risk factors include smoking, age (over 60 years old), hypertension, atherosclerosis, and male gender [2,3]. Naturally, the size of an AAA will progressively enlarge and could ultimately result in a significant mortality risk upon rupture [4].

Diagnosing AAA poses a challenge since it typically manifests without symptoms and cannot be detected through a mere physical examination [5]. As the aortic diameter grows, the risk of AAA rupture increases [6]. AAA rupture leads to severe internal bleeding, resulting in an approximately 80% mortality rate [7]. Ultrasound screening of high-risk populations, specifically men aged 65 and older, has proven to be an effective approach in preventing AAA-related mortality [8,9]. However, it is a costly method and may not be suitable for assessing AAA progression. Treatment options for patients with large (≥55 mm), rapidly growing (>10 mm), or symptomatic AAAs primarily involve endovascular exclusion or open surgery [10], with the postsurgical mortality rate for emergency operations hovering around 50% [11]. Patients with small AAAs (<55 mm) do not benefit from surgical repair [5]. Although new potential therapies have been recently proposed for AAA treatment, including nanoparticles loaded with antihypertensive drugs, statins or inhibitors of vascular endothelial growth factor receptor (VEGFR) [12,13], the current standard of care is still mostly limited

* Corresponding author.
E-mail address: lawson4001@zju.edu.cn (Z. Liu).

https://doi.org/10.1016/j.csbj.2023.10.052
Received 20 July 2023; Received in revised form 30 October 2023; Accepted 30 October 2023
Available online 2 November 2023
2001-0370/© 2023 The Author(s). Published by Elsevier B.V. on behalf of Research Network of Computational and Structural Biotechnology. This is an open access article under the CC BY-NC-ND license (http://creativecommons.org/licenses/by-nc-nd/4.0/).

to surgery at late stages of the disease. Despite progress in endovascular surgery, a definitive pharmacological treatment for AAA remains elusive, highlighting the importance of further exploring its underlying pathological mechanisms [14,15].

Abdominal aortic aneurysm (AAA) exhibits a range of pathological characteristics, including the reduction of vascular smooth muscle cells (VSMCs), deterioration of the extracellular matrix (ECM), and the infiltration of inflammatory cells. VSMCs play a crucial role in the formation of AAA. In a healthy vessel wall, VSMCs exhibit a contractile phenotype, which helps maintain vascular tone. Mutations in genes responsible for SMC contractile proteins have been linked to AAA development. The loss of SMC contractile function can disrupt vascular tone and increase aortic wall stress, thereby promoting aneurysm formation [16,17]. ECM degradation is another significant factor in AAA development [2]. Numerous studies have shown that VSMCs actively mediate ECM degradation during AAA formation [16–18]. VSMCs produce elastin and collagen to resist vasodilation and rupture. They also regulate the integrity and degradation of ECM by releasing and maturing MMPs (matrix metalloproteinases) and the tissue inhibitor of metalloproteinases (TIMPs) [19–23]. During aneurysm formation, the breakdown of elastin triggers SMC phenotypic changes, marked by increased MMP expression [20]. MMPs, particularly MMP-2 and MMP-9, play a pivotal role in degrading the extracellular matrix and weakening the aortic vascular wall during AAA formation [21]. Inflammatory cell infiltration into the aortic wall, including T-cells, B-cells, and macrophages, is a critical feature of AAA [24–26]. The composition and activation status of these immune cells change dynamically during AAA development [27]. Activated immune cells contribute to the inflammatory environment within the aortic wall, leading to VSMC apoptosis and the subsequent destruction of the aorta, ultimately resulting in the progressive growth of AAA and the risk of rupture[28].

Observational studies have highlighted a familial trend towards AAA development among relatives of affected individuals, indicating that inflammatory genes may influence an individual's susceptibility [5,29]. Several studies have reported a high prevalence of AAA among siblings of patients with AAA [30,31]. Population-based series have found that a positive family history of AAA is associated with an approximately doubled risk of AAA compared with those without a family history [32]. In a case–control study of 98 cases of AAA and 102 controls, a positive family history was associated with an increased risk of AAA (odds ratio [OR] 4.77, 95% CI 1.26–18.1)[33]. However, there has been limited systematic investigation into the specific genes and pathways that hold substantial relevance in AAA [34]. Consequently, the identification of key genes and pathways linked to AAA would significantly advance our comprehension of its pathogenesis. The emergence of next-generation sequencing technology has empowered a thorough examination of the transcriptome, streamlining gene expression quantification and establishing it as a widely employed technique in transcriptome research [35]. In this study, we profiled the tissue-specific transcriptome of the human abdominal aortic wall using RNA-seq. Integrated bioinformatics analysis was subsequently performed to investigate the molecular alterations in human AAA tissues. Our study identified several candidate key genes and pathways associated with AAA, and the differential expression of these genes was validated.

2. Materials and methods

2.1. Sample collection and RNA-seq

The protocol for collecting human tissue samples was approved by the Institutional Review Board at Second Affiliated Hospital of Zhejiang University School of Medicine, and Zhongshan Hospital of Fudan University School of Medicine (*Data supplement 1*). Written informed consent was provided by all participants or the organ donors' legal representatives. All experiments involving human tissue samples adhered to the applicable guidelines and regulations. Control abdominal aortic wall samples were acquired from organ donors, while AAA tissue samples were obtained from patients undergoing open surgery.

Following these criteria, we collected abdominal aortic wall samples from a total of 14 individuals, including 7 patients with AAA and 7 healthy individuals as controls. Patient information for abdominal aorta samples can be found in Table S1. The transcriptome was extracted following provided instructions and underwent a series of rigorous quality control procedures. RNA-seq was conducted in accordance with relevant technical guidelines. Detailed methods for RNA extraction, preprocessing, and RNA-seq are outlined in *Data Supplement2*.

2.2. Differential expression gene analysis

We conducted differential gene expression (DEG) analysis on our RNA-seq data using Deseq2 [36], while the limma package was employed for the analysis of microarrays sourced from the Gene Expression Omnibus (GEO) database [37]. We applied Benjamini and Hochberg's method to adjust the resulting p-values to control the false discovery rate. Genes meeting the criteria of an adjusted p-value < 0.05 and $|\log2 \text{ fold change}| > 1$ were designated as differentially expressed. We utilized ggplot2 and ggrepel to create the volcano plot of DEGs and the heatmap representing the top 10 up/down-regulated genes. In this study, we employed the pheatmap R package to create a heatmap depicting the top 10 up-regulated and down-regulated DEGs. We conducted hierarchical clustering on the FPKM values of genes and applied Z-score normalization to rows.

2.3. Functional annotation analysis of DEGs

To unveil the biological functions and pathways linked to the identified DEGs, we performed Gene Ontology (GO) and Kyoto Encyclopedia of Genes and Genomes (KEGG) pathway enrichment analyses using the clusterProfiler package [38–40]. We then visualized the results through Pathview, an R package designed for pathway-based data integration and visualization [41]. ClueGO software was subsequently employed to depict the connections between KEGG pathways [42]. In this analysis, the screening threshold in ClueGO was established at an adjusted *P*-value <0.01 to pinpoint essential KEGG pathways.

2.4. PPI network construction and key genes identification

To investigate the interactions among the DEGs and identify potential key genes, we established a protein-protein interaction (PPI) network utilizing data from the STRING database [43]. This constructed PPI network was later visualized using Cytoscape Software [44]. We then calculated the top 30 significant nodes within the PPI network based on their degrees using cytohubba, an extension of Cytoscape [45]. These 30 calculated nodes were recognized as candidate key genes (hub genes) associated with AAA.

2.5. Differential expression validation of candidate genes

To confirm the differential expression of our candidate key genes, we downloaded two microarray datasets (GSE7084 and GSE57691) from the GEO database, encompassing data from AAA and normal abdominal aorta wall samples [46,47]. We then evaluated the expression levels of the top 30 hub genes within these datasets. Genes exhibiting differential expression in both our RNA-seq data and these two datasets were identified as the ultimate key genes associated with AAA.

2.6. ROC analysis

Employing the pROC package, we conducted receiver operating characteristic curve (ROC) analysis to evaluate the discriminative potential of the identified key genes [48]. The area under the curve (AUC)

was computed for each dataset, and genes with an AUC exceeding 0.7 were classified as possessing a strong discriminatory capacity for AAA.

2.7. scRNA-Seq analysis

To delve deeper into the distribution of key genes across various cell types, we downloaded GSE166676, a single-cell RNA sequencing dataset featuring human AAA and control abdominal aortic samples [28]. Subsequently, we undertook preprocessing, normalization, scaling, and cell clustering of the scRNA-seq data using the Seurat R package [49]. Single R, an R package harnessing reference transcriptomic datasets of pure cell types, was employed to identify cell populations and infer the cell type of each individual cell [50]. Following this, we assessed the expression of each key gene across different cell types.

2.8. Immunohistochemical staining

To further validate the differential expression of several key genes, we constructed tissue microarrays (TMAs) containing control and AAA samples. Each TMA slide featured 40 AAA samples and 6 control abdominal aorta samples. We conducted immunohistochemical (IHC) staining on these TMAs. The methods for TMA construction and IHC staining are described in detail in *Data Supplement1*. Diaminobenzidine (DAB) substrate was utilized for color visualization, and we captured whole-slide images using the KF-PRO-020® whole slide scanner by KFBIO (Zhejiang Province, China). The staining area of each sample was quantified using Image J.

2.9. Drug-Gene interaction analysis

We utilized DGIdb to identify potential drugs linked to the key genes we identified. DGIdb is a comprehensive drug-gene interaction database that collates, structures, and provides information on drug-gene interactions and gene druggability from various sources, including research papers, databases, and web resources [51].

3. Results and discussion

3.1. PCA analysis and DEG identification

In this study, we performed PCA analysis on the gene expression values (FPKM) for all samples. Ideally, inter-group samples should exhibit dispersion, while intra-group samples should cluster together in the PCA diagram. As illustrated in Fig. 1a, the PCA diagram reveals two distinct groups, namely the control and AAA groups. The control samples tend to form tight clusters, whereas the AAA group exhibits less pronounced clustering, possibly due to variations in patient conditions, including factors such as age, AAA diameters, smoking status, and the presence of other diseases.

A total of 1148 DEGs were identified, meeting the criteria of an adjusted p-value <0.05 and absolute log2FC >1. Among these DEGs, 631 were up-regulated and 517 were down-regulated. The volcano plot in Fig. 1b illustrates the DEGs, with up-regulated genes in red dots and down-regulated genes in green dots, while genes with no significant expression change are represented as gray dots. The top 10 up-regulated

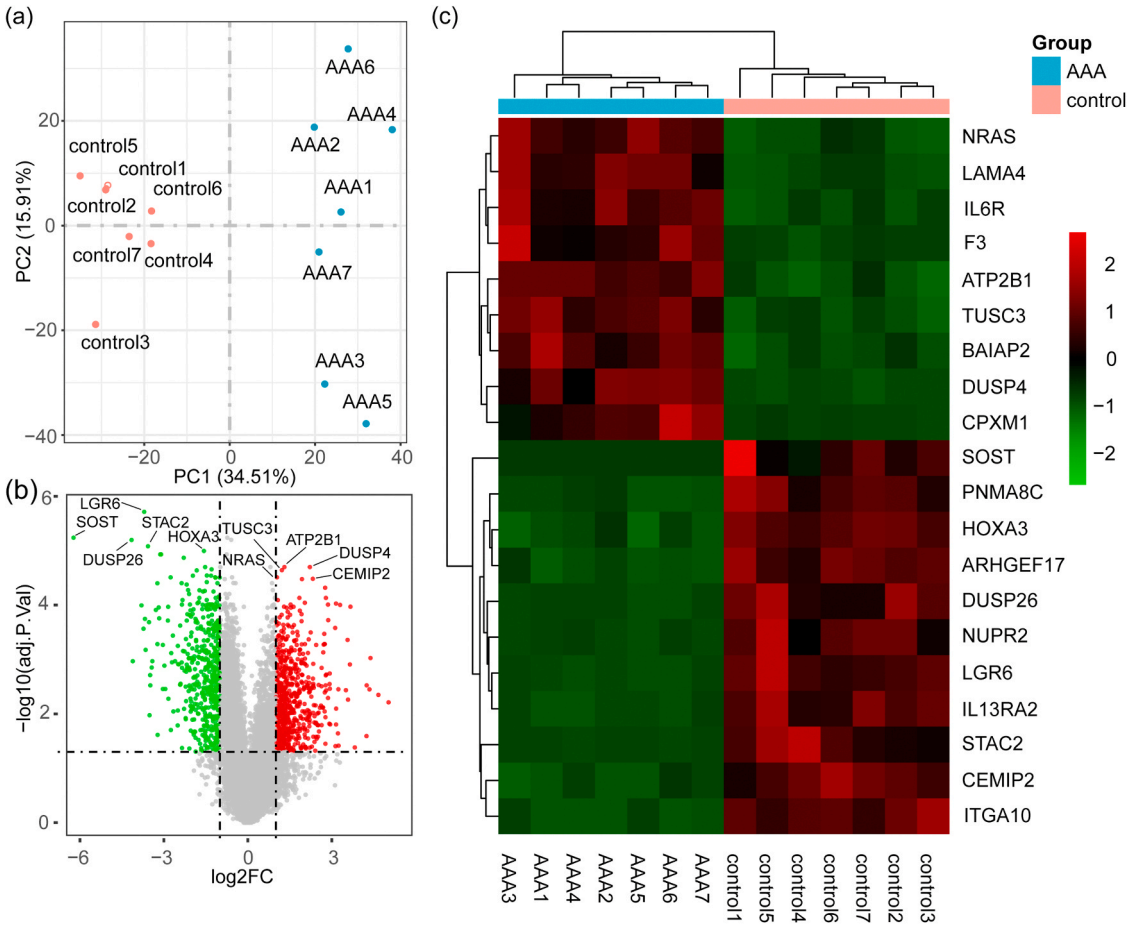

Fig. 1. DEG analysis of our RNA-Seq data. (a) PCA analysis of patients' data. (b) Volcano plot showing the results of our DEG analysis, with the top 5 up-regulated and down-regulated DEGs labeled. (c) Heatmap indicating top 10 up/down regulated DEGs. In the heatmap, red colors represent relative high gene expression levels, while green colors represent relative low gene expression levels. For interpretation of the references to color in this figure legend , the reader is referred to the web version of this article.

and down-regulated DEGs are presented in Table S2, and a heatmap of these DEGs is shown in Fig. 1c.

3.2. GO and KEGG analysis

To gain insight into the biological classification of the identified DEGs, we conducted gene ontology (GO) and Kyoto Encyclopedia of Genes and Genomes (KEGG) pathway enrichment analyses. Fig. 2a displays the enrichment analysis results for biological processes, which revealed that the DEGs were specifically enriched in extracellular matrix organization, extracellular structure organization, positive regulation of cell adhesion, cell-substrate adhesion, and T cell activation. The DEGs were also significantly enriched in collagen-containing extracellular matrix, focal adhesion, cell-substrate junction, external side of plasma membrane, and membrane raft as cellular components. In terms of molecular function, the DEGs were primary associated with extracellular matrix structural constituent, glycosaminoglycan binding, cytokine binding, fibronectin binding, and actin binding. The length of bars represents enrichment score of each GO term, which was calculated by enrichplot R package. The top 10 GO terms for biological processes, cellular components, and molecular functions are listed in Table S3.

Extracellular matrix (ECM) degradation plays a significant role in AAA pathology, which is evident from the investigation of several GO terms associated with ECM in this study. These findings underscore the critical involvement of the ECM in AAA formation, aligning with prior research.

In the KEGG pathway analysis, we identified several significant pathways, including hematopoietic cell lineage, ECM-receptor interaction, cytokine-cytokine receptor interaction, chemokine signaling pathway, and cell adhesion molecules (CAMs). The size of the circle indicates the number of DEGs enriched in a pathway, and the color of the circles represents the enrichment p-value of DEGs in each pathway. Red colors indicate relatively high enrichment p-values, while blue colors denote relatively low enrichment p-values. The X-axis represents the enrichment score of each pathway. The top 10 significant KEGG pathways are visually presented in Fig. 2b and detailed in Table S4. Additionally, Fig. 2c offers a graphical representation of the interaction between several representative genes and these top 10 KEGG pathways. In Fig. 2c, each color represents a significant KEGG pathway, and the lines within the figure illustrate the interaction of DEGs with these KEGG pathways.

Furthermore, we established an interaction network among these KEGG pathways using the clueGO software (as depicted in Fig. S1a). Several DEGs, such as *MMP9*, *CXCL2*, *THBS4*, and *CCR7*, were identified

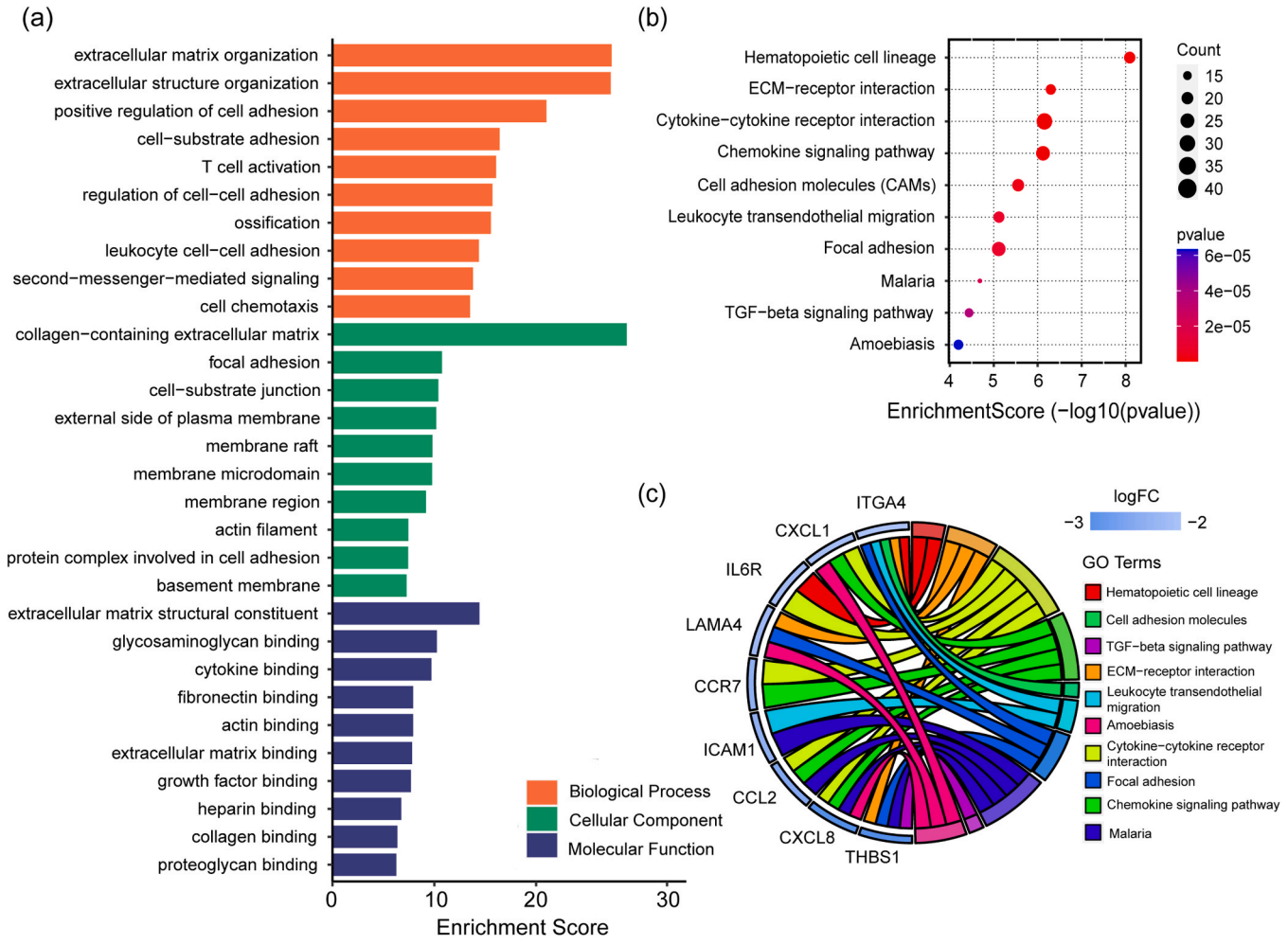

Fig. 2. Enrichment analysis of identified DEGs. (a) Top 10 Gene Ontology (GO) terms related to Biological Process (BP), Cellular Component (CC), and Molecular Function (MF). The length of the bars reflects the enrichment score of each GO term, calculated using the enrichplot R package. (b)Top 10 KEGG pathways associated with DEGs. The size of the circle represents the number of DEGs enriched in a pathway, and the color of circles represents enrichment *P*-value of DEGs in each pathway. Red colors represent relative high enrichment p-values, while blue colors represent relative low enrichment *P*-values. The X-axis represent enrichment score of each pathway. (c) The interactions between significant KEGG pathways and representative genes. Each color corresponds to a significant KEGG pathway, and the lines in the figure depict the interactions between DEGs and these pathways. For interpretation of the references to color in this figure legend , the reader is referred to the web version of this article.

as participants in multiple pathways, underscoring their significance in the development of AAA.

3.3. Construction of PPI network and identification of hub genes

We employed the STRING database to construct a protein-protein interaction (PPI) network for the purpose of examining the interactions among differentially expressed genes (DEGs) and pinpointing pivotal genes. To enhance clarity, we excluded isolated genes that lacked interactions with other genes, resulting in the depiction of the PPI network of DEGs, illustrated in Fig. S1b. Within this network, nodes symbolize proteins encoded by DEGs, while edges represent their protein interactions. We further assessed the network by ranking the top 30 nodes based on their degrees using cytoHubba, designating these nodes as potential key genes or hub genes in the context of AAA, as shown in Fig. 3a. Each dot on the graph represents a hub gene, with the colors indicating their significance. Red dots signify high significance among the hub genes, while yellow dots represent relatively lower significance. The lines connecting these dots denote interactions between proteins encoded by these genes.

3.4. Validation of hub genes by GEO datasets

To further validate the hub genes, we obtained two datasets (GSE7084 and GSE57691) from the GEO database, which contained gene expression data for AAA and control tissues (Table S2). We assessed the differential expression of the top 30 hub genes within these two datasets. Remarkably, six genes (CXCL8, CCL2, PTGS2, SELL, CCR7, and CXCL1) exhibited differential expression in both datasets, as illustrated in Fig. 3b. Consequently, these genes were designated as the definitive key genes for AAA in our study. The expression of these genes in our RNA-seq dataset is depicted in Fig. 3c and d. Both the size and color of data points in these figures reflect the gene expression levels in each sample. In Fig. 3c, dark blue signifies higher expression, while light blue represents lower expression. In Fig. 3d, red color indicates higher expression, while green indicates lower expression. Further information about these genes was illustrated in Fig. 3e.

Compared with normal aortas, both genes were found to be up regulated in AAA samples. The upregulation of these genes in AAA samples were further confirmed in the other two GEO datasets. While the precise functions of these genes in AAA development have not been comprehensively documented, prior research has implicated these key genes in various pathological processes, notably inflammation. CCL2 is a cytokine involved in immunoregulation and inflammatory processes, exhibiting chemotactic activity for monocytes and links to diseases characterized by monocyte infiltrates [52]. Given that monocyte infiltration is observed in AAA pathology, a strong connection between CCL2 and AAA is evident [53,54]. CCR7 plays a role in activating B and T lymphocytes, regulating memory T cell migration, balancing T cell responses, and promoting dendritic cell maturation in various diseases [55–58]. Notably, the infiltration and activation of T and B cells are also observed in AAA, underscoring the significance of CCR7 in AAA development [59,60]. CXCL1 and CXCL8 are members of the CXC chemokine family, which play an essential role in inflammation [61,62]. Prior studies have linked these chemokines to various cardiovascular diseases, including coronary artery disease, endothelial dysfunction, and hypertension [63–67]. PTGS2, regulated by diverse stimuli, is responsible for proteinoid biosynthesis during inflammation [68,69]. Recent research emphasizes the protective role of regulatory T cells against AAA by suppressing PTGS2 expression, highlighting PTGS2's importance in AAA development [70]. *SELL*, encoding selectin L, a cell surface adhesion molecule, is vital for leukocyte binding and rolling on endothelial cells, facilitating their migration into inflamed areas [71]. Studies have suggested that L-selectin-mediated neutrophil recruitment is an early and crucial step in AAA formation, signifying the potential significance of *SELL* in AAA [72,73]. In summary, these key genes are primarily associated with immune responses and inflammation in AAA pathology [52].

3.5. ROC analysis of identified key genes

To evaluate the discriminative potential of the identified key genes, we generated receiver operating characteristic (ROC) curves for the six key genes we identified, as depicted in Fig. 4. We calculated the area under the curve (AUC) for each dataset, and genes with an AUC exceeding 0.7 were deemed to possess a substantial discriminatory capacity in distinguishing between AAA and control abdominal aorta tissues.

As illustrated in Fig. 4, the identified key genes demonstrated notable AUC values in three datasets, including our RNA-seq data, GSE7084, and GSE57691, signifying their robust discriminatory ability.

3.6. Single-cell RNA sequencing data analysis

Following data preprocessing, normalization, scaling, and cell clustering, the dataset revealed 14 distinct clusters, as illustrated in Fig. 5a. These clusters were subsequently categorized into seven well-defined cell populations, including endothelial cells, epithelial cells, monocytes, fibroblasts, B cells, T cells, and tissue stem cells, as displayed in Fig. 5b.

In comparison to normal abdominal aortas, human AAAs exhibited an increased presence of inflammatory cells such as B cells, T cells, and monocytes, a pattern consistent with AAA pathology, as demonstrated in Fig. 5c. Furthermore, we scrutinized the expression of the identified key genes within each cell type. As portrayed in Fig. 5d, CCR7 and SELL were predominantly expressed in B cells and T cells, while CCL2 was observed in endothelial cells, fibroblasts, and tissue stem cells. PTGS2 expression was associated with endothelial cells and monocytes, and CXCL1 expression was linked to epithelial cells, fibroblasts, and monocytes.

3.7. Immunohistochemistry

To further validate the expression of specific key genes, we created tissue microarrays containing samples from normal abdominal aortas and AAAs, followed by immunohistochemical staining. The results confirmed our earlier observations, showing a substantial upregulation of CXCL8, PTGS2, SELL, CCR7, and CXCL1 in AAA when compared to control abdominal aorta samples, as depicted in Fig. 6a–e.

3.8. Drug-Gene interaction analysis

Via DGIdb, we identified 26 potential drugs linked to our key genes, with comprehensive drug information available in Data Supplementary 3. As illustrated in Fig. 6f, these drugs predominantly interact with four genes (*CXCL8*, *PTGS2*, *CCL2*, and *SELL*).

4. Conclusion and outlook

In this study, we identified six key genes (*CCL2*, *CCR7*, *CXCL1*, *CXCL8*, *PTGS2*, and *SELL*) in the pathogenesis of AAA. Our study provides a comprehensive insight into the alterations in the gene expression profile in AAA, enhancing our understanding of AAA formation and progression.

Several studies have delved into the exploration of potential key genes in AAA through integrated bioinformatics analysis. Liu et al., utilizing GSE7084 data, identified CANX, CD44, DAXX, and STAT1 as potentially significant in AAA [74]. Meanwhile, Li et al. conducted a comprehensive analysis of microarray data from GSE7084, GSE57691, and GSE47472, revealing potential key genes such as NELL2, MGAM, FOXO1, and PDGFA [75]. Additionally, Chen et al., through WCGNA analysis, pinpointed essential genes in AAA, including YIPF6, RABGAP1, ANKRD6, GPD1L, PGRMC2, HIGD1A, GMDS, MGP, SLC25A4, and

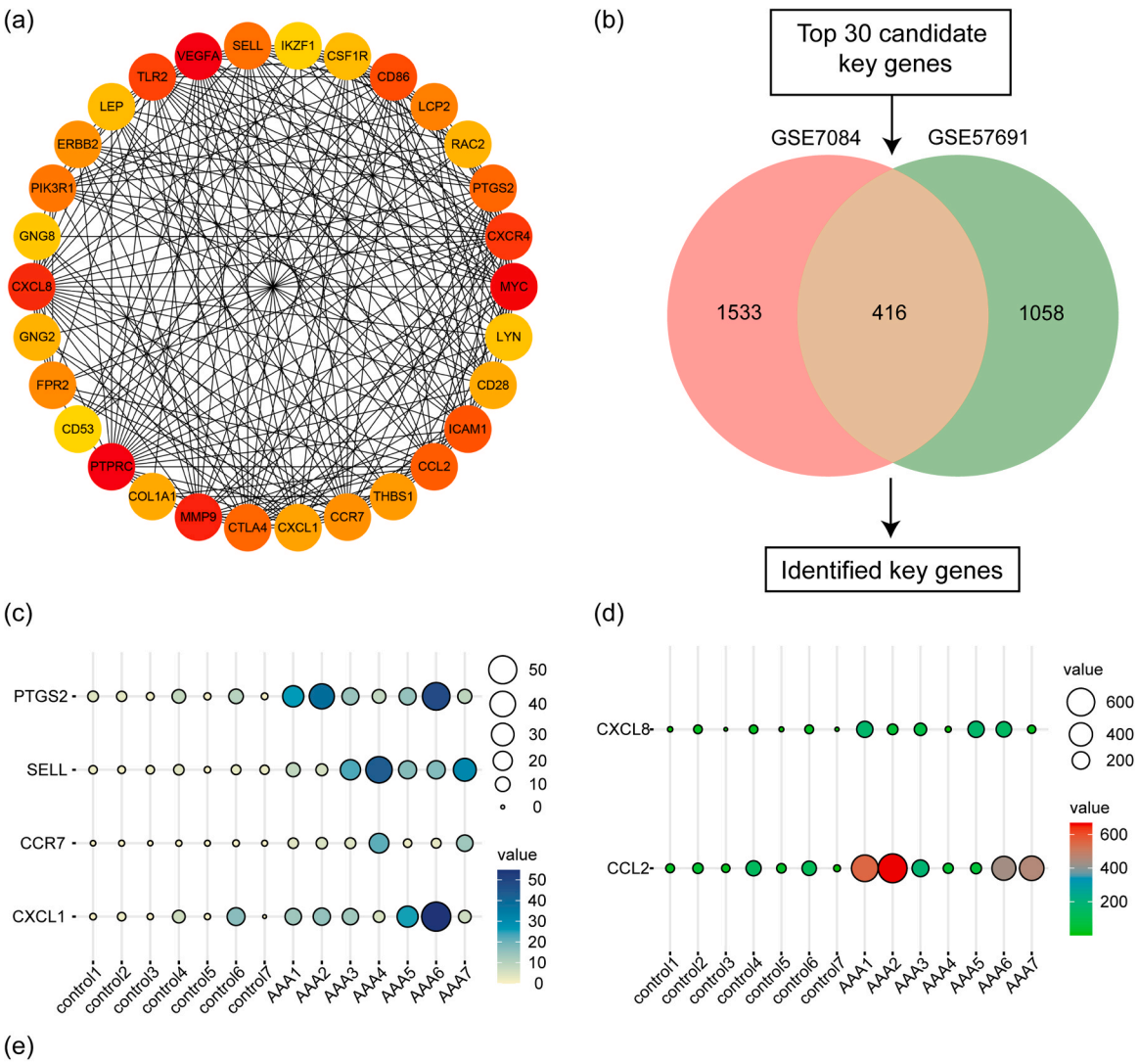

(e)

Gene ID	Gene symbol	Official full name	Log_2FC	Adj. P. Val
ENSG00000169429	CXCL8	C-X-C motif chemokine ligand 8	3.130	0.039
ENSG00000108691	CCL2	C-C motif chemokine ligand 2	2.460	0.028
ENSG00000073756	PTGS2	prostaglandin -endoperoxide synthase 2	2.188	0.009
ENSG00000188404	SELL	selectin L	2.635	0.001
ENSG00000126353	CCR7	C-C motif chemokine receptor 7	2.212	0.004
ENSG00000163739	CXCL1	C-X-C motif chemokine ligand 1	2.337	0.026

Fig. 3. Identification of potential key genes. (a) Top 30 hub genes ranked by their degree in the protein-protein interaction network of DEGs. Each dot represents a hub gene, and the colors of dots indicates the significance of hub genes. Red colors represent relative high significance of hub genes, while yellow colors represent relative low degrees of hub genes. The lines represent interactions between proteins encoded by these genes. (b) Validation of differential expression patterns of hub genes in two additional microarray datasets from the GEO database. This validation was performed to enhance the reliability of the final key gene selection. (c-d) Expression levels of final key genes in our RNA-Seq data. Both the size and color represent the expression level of these genes in each sample. In Fig. 3c, dark blue represents higher expression level, while light blue represents lower expression level. In Fig. 3d, red color represents higher expression level, while green color represents lower expression level. (e) Detailed information and expression profiles of the final identified key genes. For interpretation of the references to color in this figure legend , the reader is referred to the web version of this article.

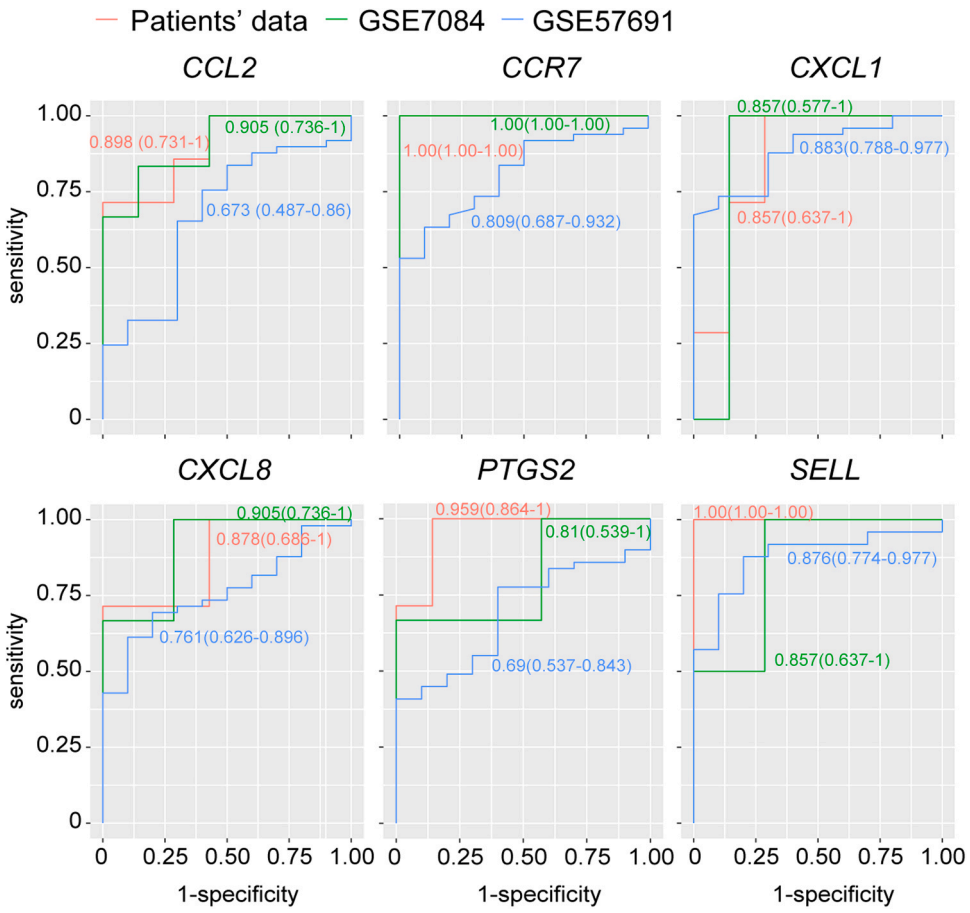

Fig. 4. ROC analysis of identified key genes. The red curve corresponds to the patients' data in our study, the green curve to the GSE7084 dataset, and the blue curve to the GSE57691 dataset. The AUC area for each curve is displayed alongside it, using the corresponding color. For interpretation of the references to color in this figure legend , the reader is referred to the web version of this article.

FAM129A [76]. Su et al., analyzing datasets from the GEO database, identified several hub genes, such as VAMP8, PTPRC, and DYNLL1 [77]. For our study, aneurysm sac samples were chosen, as the gene expression profile in aneurysm sacs holds particular relevance for investigation. We further bolstered the reliability of our findings by validating our results using GSE7084 and GSE57681 [74]. The six key genes we identified exhibited significant differential expression in two additional datasets containing normal abdominal aortas and AAA samples (GSE7084 and GSE57691). However, there was no overlap between our identified key genes and those found in other studies. This underlines the variation in the selection of key genes when different analytical processes are used. To enhance the reliability of our results, we introduced IHC experiments to further validate the differential expression of these six key genes.

Our study has certain limitations. Firstly, the relatively small number of collected abdominal aorta samples for RNA-seq may impact the precision and dependability of our findings. The advent of endovascular surgery has significantly reduced the use of traditional surgical methods for obtaining AAA samples. Recent studies indicate that approximately 80% of AAA patients undergo endovascular treatment, specifically endovascular aortic repair (EVAR). Open surgery, known as open aneurysm repair (OAR), is typically reserved for patients with a longer life expectancy and lower morbidity [10]. Consequently, our ability to collect samples through open surgery is limited, resulting in a smaller sample size. Secondly, control abdominal aorta samples were collected from patients diagnosed with cerebral hemorrhage or craniocerebral trauma. While these patients did not exhibit AAAs, molecular changes in the abdominal aorta related to their specific medical conditions might have taken place. Thirdly, more clinical differences between patients with AAA, such as age, sex, associated atherosclerotic diseases, familiarity, risk factors etc., should be taken into consideration. Additionally, expression data of serum samples were not thoroughly analyzed. Further attempts, such as ELISA quantification of the key genes in serum samples, should be made to evaluate the diagnostic value of the identified key genes. Tables 1 and 2.

5. Declarations

5.1. Ethics approval and consent for participation

The protocol for collecting human tissue samples was approved by the Institutional Review Board at the Second Affiliated Hospital of Zhejiang University School of Medicine and Zhongshan Hospital of Fudan University. Written informed consent was obtained from all participants or the legal representatives of organ donors. All experiments involving human tissue samples adhered to the applicable guidelines and regulations.

Data Availability Statement

Our RNA-seq data has been deposited in the GEO database with the accession number GSE183464. The publicly available datasets analyzed in this study (GSE7084, GSE57691, GSE166676) can be found in the GEO database.

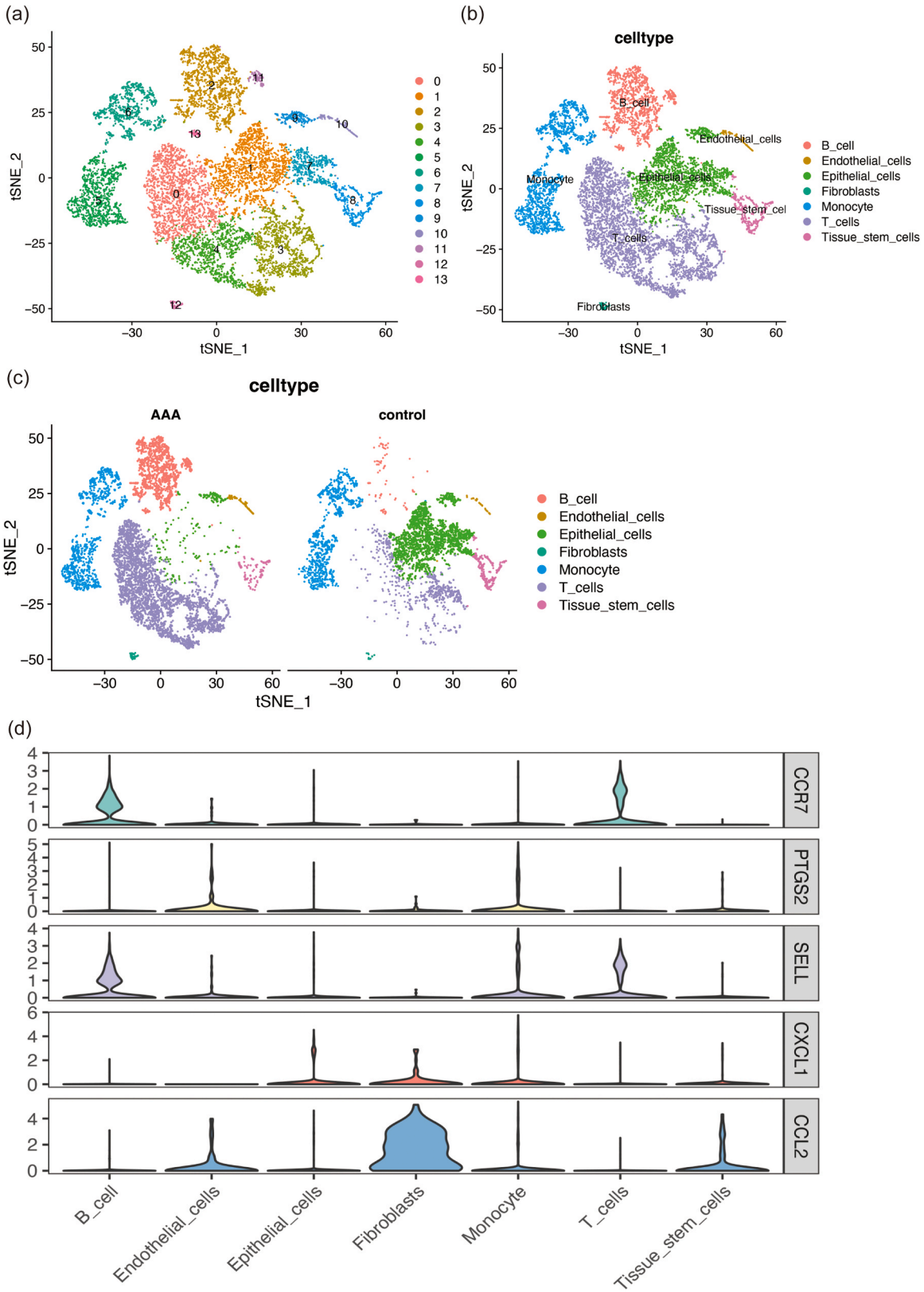

Fig. 5. Analysis of single-cell RNA-seq dataset. (a) Following preprocessing, normalization, scaling, and cell clustering, we identified a total of 14 clusters in the single-cell RNA-seq dataset. (b) These clusters were further classified into seven distinct cell populations, encompassing endothelial cells, epithelial cells, monocytes, fibroblasts, B cells, T cells, and tissue stem cells. (c) Comparison of cell-type patterns between normal abdominal aortas and Abdominal Aortic Aneurysms (AAAs). (d) Expression levels of identified key genes in various cell types.

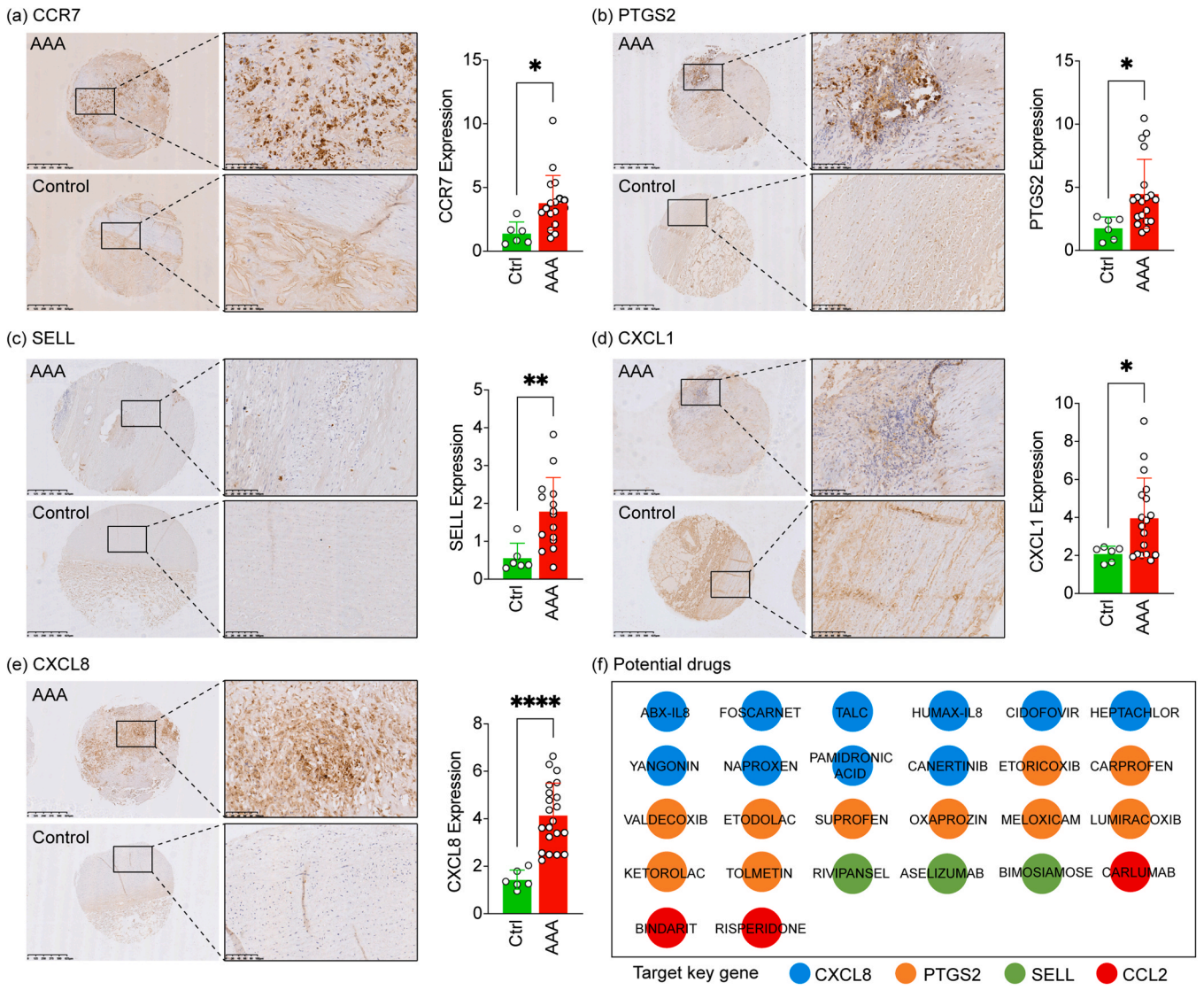

Fig. 6. (a–e) Immunohistochemistry staining of tissue microarrays (TMAs) from AAAs and normal aortas. This analysis revealed up-regulation in the protein levels of the five specified key genes: *CCR7*, *SELL*, *CXCL8*, *CXCL1*, and *PTGS2*. (f) Potential drugs associated with these key genes as indicated by DGIdb.

Table 1
Information of identified key genes.

Gene ID	Gene symbol	Official full name	Log_2FC	Adj. P Val
ENSG00000169429	CXCL8	C-X-C motif chemokine ligand 8	3.130	0.039
ENSG00000108691	CCL2	C-C motif chemokine ligand 2	2.460	0.028
ENSG00000073756	PTGS2	prostaglandin-endoperoxide synthase 2	2.188	0.009
ENSG00000188404	SELL	selectin L	2.635	0.001
ENSG00000126353	CCR7	C-C motif chemokine receptor 7	2.212	0.004
ENSG00000163739	CXCL1	C-X-C motif chemokine ligand 1	2.337	0.026

FC, fold change; Adj. P Val, adjust P value.

Table 2
ROC analysis of identified key genes.

Gene symbol	AUC (±95% CI)		
	Patients' data	GSE7084	GSE57691
CCL2	0.898 (0.731–1)	0.905 (0.736–1)	0.673 (0.487–0.86)
CCR7	1.00 (1.00–1.00)	1.00 (1.00–1.00)	0.809 (0.687–0.932)
CXCL1	0.857 (0.637–1)	0.857 (0.577–1)	0.883 (0.788–0.977)
CXCL8	0.878 (0.686–1)	0.905 (0.736–1)	0.761 (0.626–0.896)
PTGS2	0.959 (0.864–1)	0.81 (0.539–1)	0.69 (0.537–0.843)
SELL	1.00 (1.00–1.00)	0.857 (0.637–1)	0.876 (0.774–0.977)

ROC, receiver operating characteristic curve; AUC, area under curve.

Author contributions

Kaijie Zhang, Jianing Yue, and Li Yin contributed to Conceptualization, Data Curation, Formal analysis, Original Draft, and Review & Editing. **Jinyi Chen, Yunlu Chen, and Lanting Hu** contributed to the Data Curation. **Jian Shen** contributed to the Formal analysis. **Naiji Yu and Yunxia Gong** contributed to Review & Editing. **Zhenjie Liu** contributed to the Conceptualization and Review & Editing.

Funding

This work was supported by the National Natural Science Foundation of China (Grant No. 81970398), Science Fundation for Distinguished Young Scholars of Zhejiang Province (Grant No. LR22H020002), and the

Natural Science Foundation of Zhejiang Province (Grant No. Q20H020059).

Declaration of Competing Interest

The authors declare that there are no commercial or financial relationships that could be perceived as a potential conflict of interest in relation to this research.

Appendix A. Supporting information

Supplementary data associated with this article can be found in the online version at doi:10.1016/j.csbj.2023.10.052.

References

[1] Tsao CW, Aday AW, Almarzooq ZI, Anderson CAM, Arora P, Avery CL, et al. Heart disease and stroke statistics-2023 update: a report from the American Heart Association. Circulation 2023;147(8):93–621.
[2] Nordon IM, Hinchliffe RJ, Loftus IM, Thompson MM. Pathophysiology and epidemiology of abdominal aortic aneurysms. Nat Rev Cardiol 2011;8(2):92–102.
[3] Altobelli E, Rapacchietta L, Profeta VF, Fagnano R. Risk factors for abdominal aortic aneurysm in population-based studies: a systematic review and meta-analysis. Int J Environ Res Public Health 2018;15(12):2805.
[4] Karthikesalingam A, Vidal-Diez A, Holt PJ, Loftus IM, Schermerhorn ML, Soden PA, et al. Thresholds for abdominal aortic aneurysm repair in England and the United States. N Engl J Med 2016;375(21):2051–9.
[5] Sakalihasan N, Michel JB, Katsargyris A, Kuivaniemi H, Defraigne JO, Nchimi A, et al. Abdominal aortic aneurysms. Nat Rev Dis Prim 2018;4(1):1–22.
[6] Moll FL, Powell JT, Fraedrich G, Verzini F, Haulon S, Waltham M, et al. Management of abdominal aortic aneurysms clinical practice guidelines of the European society for vascular surgery. Eur J Vasc Endovasc Surg 2011;41(Suppl 1): S1–s58.
[7] Eickhoff JH. Incidence of diagnosis, operation and death from abdominal aortic aneurysms in Danish hospitals: results from a nation-wide survey, 1977-1990. Eur J Surg 1993;159(11–12):619–23.
[8] Earnshaw JJ, Lees T. Update on screening for abdominal aortic aneurysm. Eur J Vasc Endovasc Surg 2017;54(1):1–2.
[9] O'Donnell TFX, Landon BE, Schermerhorn ML. AAA screening should be expanded. Circulation 2019;140(11):889–90.
[10] Anderson PL, Arons RR, Moskowitz AJ, Gelijns A, Magnell C, Faries PL, et al. A statewide experience with endovascular abdominal aortic aneurysm repair: rapid diffusion with excellent early results. J Vasc Surg 2004;39(1):10–9.
[11] Hallin A, Bergqvist D, Holmberg L. Literature review of surgical management of abdominal aortic aneurysm. Eur J Vasc Endovasc Surg 2001;22(3):197–204.
[12] Cheng J, Zhang R, Li C, Tao H, Dou Y, Wang Y, et al. A targeting nanotherapy for abdominal aortic aneurysms. J Am Coll Cardiol 2018;72(21):2591–605.
[13] Yin L, Zhang K, Sun Y, Liu Z. Nanoparticle-assisted diagnosis and treatment for abdominal aortic aneurysm. Front Med 2021;(8):665846.
[14] Wanhainen A, Mani K, Golledge J. Surrogate markers of abdominal aortic aneurysm progression. Arterioscler Thromb Vasc Biol 2016;36(2):236–44.
[15] Kent KC. Clinical practice. Abdominal aortic aneurysms. N Engl J Med 2014;371 (22):2101–8.
[16] López-Candales A, Holmes DR, Liao S, Scott MJ, Wickline SA, Thompson RW. Decreased vascular smooth muscle cell density in medial degeneration of human abdominal aortic aneurysms. Am J Pathol 1997;150(3):993–1007.
[17] Ailawadi G, Moehle CW, Pei H, Walton SP, Yang Z, Kron IL, et al. Smooth muscle phenotypic modulation is an early event in aortic aneurysms. J Thorac Cardiovasc Surg 2009;138(6):1392–9.
[18] Kuivaniemi H, Ryer EJ, Elmore JR, Tromp G. Understanding the pathogenesis of abdominal aortic aneurysms. Expert Rev Cardiovasc Ther 2015;13(9):975–87.
[19] Mazurek R, Dave JM, Chandran RR, Misra A, Sheikh AQ, Greif DM. Vascular cells in blood vessel wall development and disease. Adv Pharm 2017;78:323–50.
[20] van Varik BJ, Rennenberg RJ, Reutelingsperger CP, Kroon AA, de Leeuw PW, Schurgers LJ. Mechanisms of arterial remodeling: lessons from genetic diseases. Front Genet 2012;3:1–10.
[21] Bendeck MP, Irvin C, Reidy MA. Inhibition of matrix metalloproteinase activity inhibits smooth muscle cell migration but not neointimal thickening after arterial injury. Circ Res 1996;78(1):38–43.
[22] Tilson MD, Reilly JM, Brophy CM, Webster EL, Barnett TR. Expression and sequence of the gene for tissue inhibitor of metalloproteinases in patients with abdominal aortic aneurysms. J Vasc Surg 1993;18(2):266–70.
[23] Raffetto JD, Khalil RA. Matrix metalloproteinases and their inhibitors in vascular remodeling and vascular disease. Biochem Pharm 2008;75(2):346–59.
[24] Koch AE, Haines GK, Rizzo RJ, Radosevich JA, Pope RM, Robinson PG, et al. Human abdominal aortic aneurysms. immunophenotypic analysis suggesting an immune-mediated response. Am J Pathol 1990;137(5):1199–213.
[25] Gregory AK, Yin NX, Capella J, Xia S, Newman KM, Tilson MD. Features of autoimmunity in the abdominal aortic aneurysm. Arch Surg 1996;131(1):85–8.
[26] Yuan Z, Lu Y, Wei J, Wu J, Yang J, Cai Z. Abdominal aortic aneurysm: roles of inflammatory cells. Front Immunol 2020;11:609161.
[27] Raffort J, Lareyre F, Clément M, Hassen-Khodja R, Chinetti G, Mallat Z. Monocytes and macrophages in abdominal aortic aneurysm. Nat Rev Cardiol 2017;14(8): 457–71.
[28] Davis FM, Tsoi LC, Melvin WJ, denDekker A, Wasikowski R, Joshi AD, et al. Inhibition of macrophage histone demethylase JMJD3 protects against abdominal aortic aneurysms. J Exp Med 2021;218(6):e20201839.
[29] Sandford RM, Bown MJ, London NJ, Sayers RD. The genetic basis of abdominal aortic aneurysms: a review. Eur J Vasc Endovasc Surg 2007;33(4):381–90.
[30] Ogata T, MacKean GL, Cole CW, Arthur C, Andreou P, Tromp G, et al. The lifetime prevalence of abdominal aortic aneurysms among siblings of aneurysm patients is eightfold higher than among siblings of spouses: an analysis of 187 aneurysm families in Nova Scotia, Canada. J Vasc Surg 2005;42(5):891–7.
[31] Clifton MA. Familial abdominal aortic aneurysms. Br J Surg 1977;64(11):765–6.
[32] Larsson E, Granath F, Swedenborg J, Hultgren R. A population-based case-control study of the familial risk of abdominal aortic aneurysm. J Vasc Surg 2009;49(1): 47–50.
[33] Blanchard JF, Armenian HK, Friesen PP. Risk factors for abdominal aortic aneurysm: results of a case-control study. Am J Epidemiol 2000;151(6):575–83.
[34] Pinard A, Jones GT, Milewicz DM. Genetics of thoracic and abdominal aortic diseases. Circ Res 2019;124(4):588–606.
[35] Metzker ML. Sequencing technologies—the next generation. Nat Rev Genet 2010; 11(1):31–46.
[36] Love MI, Huber W, Anders S. Moderated estimation of fold change and dispersion for RNA-seq data with DESeq2. Genome Biol 2014;15(12). 550:1-21.
[37] Ritchie ME, Phipson B, Wu D, Hu Y, Law CW, Shi W, et al. limma powers differential expression analyses for RNA-sequencing and microarray studies. Nucleic Acids Res 2015;43(7):e47.
[38] Yu G, Wang LG, Han Y, He QY. clusterProfiler: an R package for comparing biological themes among gene clusters. Omics 2012;16(5):284–7.
[39] The Gene. Ontology resource: 20 years and still going strong. Nucleic Acids Res 2019;47(D1):D330–8.
[40] Kanehisa M, Goto S. KEGG: kyoto encyclopedia of genes and genomes. Nucleic Acids Res 2000;28(1):27–30.
[41] Luo W, Brouwer C. Pathview: an R/Bioconductor package for pathway-based data integration and visualization. Bioinformatics 2013;29(14):1830–1.
[42] Bindea G, Mlecnik B, Hackl H, Charoentong P, Tosolini M, Kirilovsky A, et al. ClueGO: a Cytoscape plug-in to decipher functionally grouped gene ontology and pathway annotation networks. Bioinforma 2009;25(8):1091–3.
[43] Szklarczyk D, Gable AL, Nastou KC, Lyon D, Kirsch R, Pyysalo S, et al. The STRING database in 2021: customizable protein-protein networks, and functional characterization of user-uploaded gene/measurement sets. Nucleic Acids Res 2021; 49(D1):D605–d12.
[44] Shannon P, Markiel A, Ozier O, Baliga NS, Wang JT, Ramage D, et al. Cytoscape: a software environment for integrated models of biomolecular interaction networks. Genome Res 2003;13(11):2498–504.
[45] Chin CH, Chen SH, Wu HH, Ho CW, Ko MT, Ko MT. cytoHubba: identifying hub objects and sub-networks from complex interactome. BMC Syst Biol 2014;8(Suppl 4):S11. Suppl 4:1-7.
[46] Lenk GM, Tromp G, Weinsheimer S, Gatalica Z, Berguer R, Kuivaniemi H. Whole genome expression profiling reveals a significant role for immune function in human abdominal aortic aneurysms. BMC Genom 2007;8. 237:1 12.
[47] Biros E, Gäbel G, Moran CS, Schreurs C, Lindeman JH, Walker PJ, et al. Differential gene expression in human abdominal aortic aneurysm and aortic occlusive disease. Oncotarget 2015;6(15):12984–96.
[48] Robin X, Turck N, Hainard A, Tiberti N, Lisacek F, Sanchez JC, et al. pROC: an open-source package for R and S+ to analyze and compare ROC curves. BMC Bioinforma 2011;12:1–8.
[49] Butler A, Hoffman P, Smibert P, Papalexi E, Satija R. Integrating single-cell transcriptomic data across different conditions, technologies, and species. Nat Biotechnol 2018;36(5):411–20.
[50] Aran D, Looney AP, Liu L, Wu E, Fong V, Hsu A, et al. Reference-based analysis of lung single-cell sequencing reveals a transitional profibrotic macrophage. Nat Immunol 2019;20(2):163–72.
[51] Cotto KC, Wagner AH, Feng YY, Kiwala S, Coffman AC, Spies G, et al. DGIdb 3.0: a redesign and expansion of the drug-gene interaction database. Nucleic Acids Res 2018;46(D1):D1068–73.
[52] O'Connor T, Borsig L, Heikenwalder M. CCL2-CCR2 signaling in disease pathogenesis. Endocr Metab Immune Disord Drug Targets 2015;15(2):105–18.
[53] Liu Z, Morgan S, Ren J, Wang Q, Annis DS, Mosher DF, et al. Thrombospondin-1 (TSP1) contributes to the development of vascular inflammation by regulating monocytic cell motility in mouse models of abdominal aortic aneurysm. Circ Res 2015;117(2):129–41.
[54] Jiang H, Sasaki T, Jin E, Kuzuya M, Cheng XW. Inflammatory cells and proteases in abdominal aortic aneurysm and its complications. Curr Drug Targets 2018;19(11): 1289–96.
[55] Moschovakis GL, Förster R. Multifaceted activities of CCR7 regulate T-cell homeostasis in health and disease. Eur J Immunol 2012;42(8):1949–55.
[56] Förster R, Davalos-Misslitz AC, Rot A. CCR7 and its ligands: balancing immunity and tolerance. Nat Rev Immunol 2008;8(5):362–71.
[57] Larsen KO, Yndestad A, Sjaastad I, Løberg EM, Goverud IL, Halvorsen B, et al. Lack of CCR7 induces pulmonary hypertension involving perivascular leukocyte infiltration and inflammation. Am J Physiol Lung Cell Mol Physiol 2011;301(1): L50–9.
[58] Zhang Y, Gao W, Yuan J, Zhong X, Yao K, Luo R, et al. CCR7 mediates dendritic-cell-derived exosome migration and improves cardiac function after myocardial infarction. Pharmaceutics 2023;15(2):461.

[59] Li J, Xia N, Wen S, Li D, Lu Y, Gu M, et al. IL (Interleukin)-33 suppresses abdominal aortic aneurysm by enhancing regulatory T-cell expansion and activity. Arterioscler Thromb Vasc Biol 2019;39(3):446–58.
[60] Zhou Y, Wu W, Lindholt JS, Sukhova GK, Libby P, Yu X, et al. Regulatory T cells in human and angiotensin II-induced mouse abdominal aortic aneurysms. Cardiovasc Res 2015;107(1):98–107.
[61] Rizas KD, Ippagunta N, Tilson 3rd MD. Immune cells and molecular mediators in the pathogenesis of the abdominal aortic aneurysm. Cardiol Rev 2009;17(5): 201–10.
[62] Tsilimigras DI, Sigala F, Karaolanis G, Ntanasis-Stathopoulos I, Spartalis E, Spartalis M, et al. Cytokines as biomarkers of inflammatory response after open versus endovascular repair of abdominal aortic aneurysms: a systematic review. Acta Pharm Sin 2018;39(7):1164–75.
[63] Zhang RJ, Li XD, Zhang SW, Li XH, Wu L. IL-8 -251A/T polymorphism contributes to coronary artery disease susceptibility in a Chinese population. Genet Mol Res 2017;16(1):1–7.
[64] Bouabdallah J, Zibara K, Issa H, Lenglet G, Kchour G, Caus T, et al. Endothelial cells exposed to phosphate and indoxyl sulphate promote vascular calcification through interleukin-8 secretion. Nephrol Dial Transpl 2019;34(7):1125–34.
[65] Wang L, Zhang YL, Lin QY, Liu Y, Guan XM, Ma XL, et al. CXCL1-CXCR2 axis mediates angiotensin II-induced cardiac hypertrophy and remodelling through regulation of monocyte infiltration. Eur Heart J 2018;39(20):1818–31.
[66] Wang S, Bai J, Zhang YL, Lin QY, Han X, Qu WK, et al. CXCL1-CXCR2 signalling mediates hypertensive retinopathy by inducing macrophage infiltration. Redox Biol 2022;56:102438.
[67] Mikolajczyk TP, Szczepaniak P, Vidler F, Maffia P, Graham GJ, Guzik TJ. Role of inflammatory chemokines in hypertension. Pharm Ther 2021;223:107799.
[68] Cornejo-García JA, Perkins JR, Jurado-Escobar R, García-Martín E, Agúndez JA, Viguera E, et al. Pharmacogenomics of Prostaglandin and Leukotriene Receptors. Front Pharm 2016;7. 316:1 9.
[69] Mitchell JA, Kirkby NS, Ahmetaj-Shala B, Armstrong PC, Crescente M, Ferreira P, et al. Cyclooxygenases and the cardiovascular system. Pharm Ther 2021;217: 107624.
[70] Molina-Sánchez P, Del Campo L, Esteban V, Rius C, Chèvre R, Fuster JJ, et al. Defective p27 phosphorylation at serine 10 affects vascular reactivity and increases abdominal aortic aneurysm development via Cox-2 activation. J Mol Cell Cardiol 2018;116:5–15.
[71] Ivetic A, Hoskins Green HL, Hart SJ. L-selectin: a major regulator of leukocyte adhesion, migration and signaling. Front Immunol 2019;10(1068):1–22.
[72] Hannawa KK, Eliason JL, Woodrum DT, Pearce CG, Roelofs KJ, Grigoryants V, et al. L-selectin-mediated neutrophil recruitment in experimental rodent aneurysm formation. Circulation 2005;112(2):241–7.
[73] Vandestienne M, Zhang Y, Santos-Zas I, Al-Rifai R, Joffre J, Giraud A, et al. TREM-1 orchestrates angiotensin II-induced monocyte trafficking and promotes experimental abdominal aortic aneurysm. J Clin Invest 2021;131(2):e142468.
[74] Liu Y, Wang X, Wang H, Hu T. Identification of key genes and pathways in abdominal aortic aneurysm by integrated bioinformatics analysis. J. Int Med Res 2020;48(4):1–13.
[75] Wan L, Huang J, Ni H, Yu G. Screening key genes for abdominal aortic aneurysm based on gene expression omnibus dataset. BMC Cardiovasc Disord 2018;18(1). 34: 1-13.
[76] Chen S, Yang D, Lei C, Li Y, Sun X, Chen M, et al. Identification of crucial genes in abdominal aortic aneurysm by WGCNA. PeerJ 2019;7:e7873.
[77] Su Z, Gu Y. Identification of key genes and pathways involved in abdominal aortic aneurysm initiation and progression. Vascular 2022;30(4):639–49.